

MIT Open Access Articles

*Search for Gluino-Mediated Bottom Squark
Production in $pp\bar{p}$ Collisions at $\sqrt{s}=1.96$ TeV*

The MIT Faculty has made this article openly available. **Please share** how this access benefits you. Your story matters.

Citation: Aaltonen, T. et al. "Search for Gluino-Mediated Bottom Squark Production in $pp\bar{p}$ Collisions at $\sqrt{s}=1.96$ TeV." Physical Review Letters 102.22 (2009): 221801. (C) 2010 The American Physical Society.

As Published: <http://dx.doi.org/10.1103/PhysRevLett.102.221801>

Publisher: American Physical Society

Persistent URL: <http://hdl.handle.net/1721.1/51353>

Version: Final published version: final published article, as it appeared in a journal, conference proceedings, or other formally published context

Terms of Use: Article is made available in accordance with the publisher's policy and may be subject to US copyright law. Please refer to the publisher's site for terms of use.



Search for Gluino-Mediated Bottom Squark Production in $p\bar{p}$ Collisions at $\sqrt{s} = 1.96$ TeV

T. Aaltonen,²⁴ J. Adelman,¹⁴ T. Akimoto,⁵⁶ B. Álvarez González,^{12,u} S. Amerio,^{44b,44a} D. Amidei,³⁵ A. Anastassov,³⁹ A. Annovi,²⁰ J. Antos,¹⁵ G. Apollinari,¹⁸ A. Apresyan,⁴⁹ T. Arisawa,⁵⁸ A. Artikov,¹⁶ W. Ashmanskas,¹⁸ A. Attal,⁴ A. Aurisano,⁵⁴ F. Azfar,⁴³ W. Badgett,¹⁸ A. Barbaro-Galtieri,²⁹ V. E. Barnes,⁴⁹ B. A. Barnett,²⁶ P. Barria,^{47c,47a} V. Bartsch,³¹ G. Bauer,³³ P.-H. Beauchemin,³⁴ F. Bedeschi,^{47a} D. Beecher,³¹ S. Behari,²⁶ G. Bellettini,^{47b,47a} J. Bellinger,⁶⁰ D. Benjamin,¹⁷ A. Beretvas,¹⁸ J. Beringer,²⁹ A. Bhatti,⁵¹ M. Binkley,¹⁸ D. Bisello,^{44b,44a} I. Bizjak,^{31,z} R. E. Blair,² C. Blocker,⁷ B. Blumenfeld,²⁶ A. Bocci,¹⁷ A. Bodek,⁵⁰ V. Boisvert,⁵⁰ G. Bolla,⁴⁹ D. Bortoletto,⁴⁹ J. Boudreau,⁴⁸ A. Boveia,¹¹ B. Brau,^{11,b} A. Bridgeman,²⁵ L. Brigliadori,^{6b,6a} C. Bromberg,³⁶ E. Brubaker,¹⁴ J. Budagov,¹⁶ H. S. Budd,⁵⁰ S. Budd,²⁵ S. Burke,¹⁸ K. Burkett,¹⁸ G. Busetto,^{44b,44a} P. Bussey,²² A. Buzatu,³⁴ K. L. Byrum,² S. Cabrera,^{17,w} C. Calancha,³² M. Campanelli,³⁶ M. Campbell,³⁵ F. Canelli,^{14,18} A. Canepa,⁴⁶ B. Carls,²⁵ D. Carlsmith,⁶⁰ R. Carosi,^{47a} S. Carrillo,^{19,o} S. Carron,³⁴ B. Casal,¹² M. Casarsa,¹⁸ A. Castro,^{6b,6a} P. Catastini,^{47c,47a} D. Cauz,^{55b,55a} V. Cavaliere,^{47c,47a} M. Cavalli-Sforza,⁴ A. Cerri,²⁹ L. Cerrito,^{31,q} S. H. Chang,²⁸ Y. C. Chen,¹ M. Chertok,⁸ G. Chiarelli,^{47a} G. Chlachidze,¹⁸ F. Chlebana,¹⁸ K. Cho,²⁸ D. Chokheli,¹⁶ J. P. Chou,²³ G. Choudalakis,³³ S. H. Chuang,⁵³ K. Chung,^{18,p} W. H. Chung,⁶⁰ Y. S. Chung,⁵⁰ T. Chwalek,²⁷ C. I. Ciobanu,⁴⁵ M. A. Ciocci,^{47c,47a} A. Clark,²¹ D. Clark,⁷ G. Compostella,^{44a} M. E. Convery,¹⁸ J. Conway,⁸ M. Cordelli,²⁰ G. Cortiana,^{44b,44a} C. A. Cox,⁸ D. J. Cox,⁸ F. Crescioli,^{47b,47a} C. Cuenca Almenar,^{8,w} J. Cuevas,^{12,u} R. Culbertson,¹⁸ J. C. Cully,³⁵ D. Dagenhart,¹⁸ M. Datta,¹⁸ T. Davies,²² P. de Barbaro,⁵⁰ S. De Cecco,^{52a} A. Deisher,²⁹ G. De Lorenzo,⁴ M. Dell'Orso,^{47b,47a} C. Deluca,⁴ L. Demortier,⁵¹ J. Deng,¹⁷ M. Deninno,^{6a} P. F. Derwent,¹⁸ A. Di Canto,^{47b,47a} G. P. di Giovanni,⁴⁵ C. Dionisi,^{52b,52a} B. Di Ruzza,^{55b,55a} J. R. Dittmann,⁵ M. D'Onofrio,⁴ S. Donati,^{47b,47a} P. Dong,⁹ J. Donini,^{44a} T. Dorigo,^{44a} S. Dube,⁵³ J. Efron,⁴⁰ A. Elagin,⁵⁴ R. Erbacher,⁸ D. Errede,²⁵ S. Errede,²⁵ R. Eusebi,¹⁸ H. C. Fang,²⁹ S. Farrington,⁴³ W. T. Fedorko,¹⁴ R. G. Feild,⁶¹ M. Feindt,²⁷ J. P. Fernandez,³² C. Ferrazza,^{47d,47a} R. Field,¹⁹ G. Flanagan,⁴⁹ R. Forrest,⁸ M. J. Frank,⁵ M. Franklin,²³ J. C. Freeman,¹⁸ I. Furic,¹⁹ M. Gallinaro,^{52a} J. Galyardt,¹³ F. Garberon,¹¹ J. E. Garcia,²¹ A. F. Garfinkel,⁴⁹ P. Garosi,^{47c,47a} K. Genser,¹⁸ H. Gerberich,²⁵ D. Gerdes,³⁵ A. Gessler,²⁷ S. Giagu,^{52b,52a} V. Giakoumopoulou,³ P. Giannetti,^{47a} K. Gibson,⁴⁸ J. L. Gimmell,⁵⁰ C. M. Ginsburg,¹⁸ N. Giokaris,³ M. Giordani,^{55b,55a} P. Giromini,²⁰ M. Giunta,^{47a} G. Giurgiu,²⁶ V. Glagolev,¹⁶ D. Glenzinski,¹⁸ M. Gold,³⁸ N. Goldschmidt,¹⁹ A. Golossanov,¹⁸ G. Gomez,¹² G. Gomez-Ceballos,³³ M. Goncharov,³³ O. González,³² I. Gorelov,³⁸ A. T. Goshaw,¹⁷ K. Goulianos,⁵¹ A. Gresele,^{44b,44a} S. Grinstein,²³ C. Grosso-Pilcher,¹⁴ R. C. Group,¹⁸ U. Grundler,²⁵ J. Guimaraes da Costa,²³ Z. Gunay-Unalan,³⁶ C. Haber,²⁹ K. Hahn,³³ S. R. Hahn,¹⁸ E. Halkiadakis,⁵³ B.-Y. Han,⁵⁰ J. Y. Han,⁵⁰ F. Happacher,²⁰ K. Hara,⁵⁶ D. Hare,⁵³ M. Hare,⁵⁷ S. Harper,⁴³ R. F. Harr,⁵⁹ R. M. Harris,¹⁸ M. Hartz,⁴⁸ K. Hatakeyama,⁵¹ C. Hays,⁴³ M. Heck,²⁷ A. Heijboer,⁴⁶ J. Heinrich,⁴⁶ C. Henderson,³³ M. Herndon,⁶⁰ J. Heuser,²⁷ S. Hewamanage,⁵ D. Hidas,¹⁷ C. S. Hill,^{11,d} D. Hirschbuehl,²⁷ A. Hocker,¹⁸ S. Hou,¹ M. Houlden,³⁰ S.-C. Hsu,²⁹ B. T. Huffman,⁴³ R. E. Hughes,⁴⁰ U. Husemann,⁶¹ M. Hussein,³⁶ J. Huston,³⁶ J. Incandela,¹¹ G. Introzzi,^{47a} M. Iori,^{52b,52a} A. Ivanov,⁸ E. James,¹⁸ D. Jang,¹³ B. Jayatilaka,¹⁷ E. J. Jeon,²⁸ M. K. Jha,^{6a} S. Jindariani,¹⁸ W. Johnson,⁸ M. Jones,⁴⁹ K. K. Joo,²⁸ S. Y. Jun,¹³ J. E. Jung,²⁸ T. R. Junk,¹⁸ T. Kamon,⁵⁴ D. Kar,¹⁹ P. E. Karchin,⁵⁹ Y. Kato,^{42,n} R. Kephart,¹⁸ W. Ketchum,¹⁴ J. Keung,⁴⁶ V. Khotilovich,⁵⁴ B. Kilminster,¹⁸ D. H. Kim,²⁸ H. S. Kim,²⁸ H. W. Kim,²⁸ J. E. Kim,²⁸ M. J. Kim,²⁰ S. B. Kim,²⁸ S. H. Kim,⁵⁶ Y. K. Kim,¹⁴ N. Kimura,⁵⁶ L. Kirsch,⁷ S. Klimentenko,¹⁹ B. Knuteson,³³ B. R. Ko,¹⁷ K. Kondo,⁵⁸ D. J. Kong,²⁸ J. Konigsberg,¹⁹ A. Korytov,¹⁹ A. V. Kotwal,¹⁷ M. Kreps,²⁷ J. Kroll,⁴⁶ D. Krop,¹⁴ N. Krumnack,⁵ M. Kruse,¹⁷ V. Krutelyov,¹¹ T. Kubo,⁵⁶ T. Kuhr,²⁷ N. P. Kulkarni,⁵⁹ M. Kurata,⁵⁶ S. Kwang,¹⁴ A. T. Laasanen,⁴⁹ S. Lami,^{47a} S. Lammel,¹⁸ M. Lancaster,³¹ R. L. Lander,⁸ K. Lannon,^{40,t} A. Lath,⁵³ G. Latino,^{47c,47a} I. Lazzizzera,^{44b,44a} T. LeCompte,² E. Lee,⁵⁴ H. S. Lee,¹⁴ S. W. Lee,^{54,v} S. Leone,^{47a} J. D. Lewis,¹⁸ C.-S. Lin,²⁹ J. Linacre,⁴³ M. Lindgren,¹⁸ E. Lipeles,⁴⁶ A. Lister,⁸ D. O. Litvintsev,¹⁸ C. Liu,⁴⁸ T. Liu,¹⁸ N. S. Lockyer,⁴⁶ A. Loginov,⁶¹ M. Loreti,^{44b,44a} L. Lovas,¹⁵ D. Lucchesi,^{44b,44a} C. Luci,^{52b,52a} J. Lueck,²⁷ P. Lujan,²⁹ P. Lukens,¹⁸ G. Lungu,⁵¹ L. Lyons,⁴³ J. Lys,²⁹ R. Lysak,¹⁵ D. MacQueen,³⁴ R. Madrak,¹⁸ K. Maeshima,¹⁸ K. Makhoul,³³ T. Maki,²⁴ P. Maksimovic,²⁶ S. Malde,⁴³ S. Malik,³¹ G. Manca,^{30,f} A. Manousakis-Katsikakis,³ F. Margaroli,⁴⁹ C. Marino,²⁷ C. P. Marino,²⁵ A. Martin,⁶¹ V. Martin,^{22,1} M. Martínez,⁴ R. Martínez-Ballarín,³² T. Maruyama,⁵⁶ P. Mastrandrea,^{52a} T. Masubuchi,⁵⁶ M. Mathis,²⁶ M. E. Mattson,⁵⁹ P. Mazzanti,^{6a} K. S. McFarland,⁵⁰ P. McIntyre,⁵⁴ R. McNulty,^{30,k} A. Mehta,³⁰ P. Mehtala,²⁴ A. Menzione,^{47a} P. Merkel,⁴⁹ C. Mesropian,⁵¹ T. Miao,¹⁸ N. Miladinovic,⁷ R. Miller,³⁶ C. Mills,²³ M. Milnik,²⁷ A. Mitra,¹ G. Mitselmakher,¹⁹ H. Miyake,⁵⁶ N. Moggi,^{6a} C. S. Moon,²⁸ R. Moore,¹⁸ M. J. Morello,^{47a} J. Morlock,²⁷ P. Movilla Fernandez,¹⁸ J. Mülmenstädt,²⁹ A. Mukherjee,¹⁸ Th. Muller,²⁷ R. Mumford,²⁶ P. Murat,¹⁸ M. Mussini,^{6b,6a} J. Nachtman,^{18,p} Y. Nagai,⁵⁶ A. Nagano,⁵⁶ J. Naganoma,⁵⁶ K. Nakamura,⁵⁶ I. Nakano,⁴¹

A. Napier,⁵⁷ V. Nečula,¹⁷ J. Nett,⁶⁰ C. Neu,^{46,x} M. S. Neubauer,²⁵ S. Neubauer,²⁷ J. Nielsen,^{29,h} L. Nodulman,² M. Norman,¹⁰ O. Norniella,²⁵ E. Nurse,³¹ L. Oakes,⁴³ S. H. Oh,¹⁷ Y. D. Oh,²⁸ I. Oksuzian,¹⁹ T. Okusawa,⁴² R. Orava,²⁴ K. Osterberg,²⁴ S. Pagan Griso,^{44b,44a} E. Palencia,¹⁸ V. Papadimitriou,¹⁸ A. Papaikonomou,²⁷ A. A. Paramonov,¹⁴ B. Parks,⁴⁰ S. Pashapour,³⁴ J. Patrick,¹⁸ G. Pauletta,^{55b,55a} M. Paulini,¹³ C. Paus,³³ T. Peiffer,²⁷ D. E. Pellett,⁸ A. Penzo,^{55a} T. J. Phillips,¹⁷ G. Piacentino,^{47a} E. Pianori,⁴⁶ L. Pinera,¹⁹ K. Pitts,²⁵ C. Plager,⁹ L. Pondrom,⁶⁰ O. Poukhov,^{16,a} N. Pounder,⁴³ F. Prakoshyn,¹⁶ A. Pronko,¹⁸ J. Proudfoot,² F. Ptohos,^{18,j} E. Pueschel,¹³ G. Punzi,^{47b,47a} J. Pursley,⁶⁰ J. Rademacker,^{43,d} A. Rahaman,⁴⁸ V. Ramakrishnan,⁶⁰ N. Ranjan,⁴⁹ I. Redondo,³² P. Renton,⁴³ M. Renz,²⁷ M. Rescigno,^{52a} S. Richter,²⁷ F. Rimondi,^{6b,6a} L. Ristori,^{47a} A. Robson,²² T. Rodrigo,¹² T. Rodriguez,⁴⁶ E. Rogers,²⁵ S. Rolli,⁵⁷ R. Roser,¹⁸ M. Rossi,^{55a} R. Rossin,¹¹ P. Roy,³⁴ A. Ruiz,¹² J. Russ,¹³ V. Rusu,¹⁸ B. Rutherford,¹⁸ H. Saarikko,²⁴ A. Safonov,⁵⁴ W. K. Sakumoto,⁵⁰ O. Saltó,⁴ L. Santi,^{55b,55a} S. Sarkar,^{52b,52a} L. Sartori,^{47a} K. Sato,¹⁸ A. Savoy-Navarro,⁴⁵ P. Schlabach,¹⁸ A. Schmidt,²⁷ E. E. Schmidt,¹⁸ M. A. Schmidt,¹⁴ M. P. Schmidt,⁶¹ M. Schmitt,³⁹ T. Schwarz,⁸ L. Scodellaro,¹² A. Scribano,^{47c,47a} F. Scuri,^{47a} A. Sedov,⁴⁹ S. Seidel,³⁸ Y. Seiya,⁴² A. Semenov,¹⁶ L. Sexton-Kennedy,¹⁸ F. Sforza,^{47b,47a} A. Sfyrla,²⁵ S. Z. Shalhout,⁵⁹ T. Shears,³⁰ P. F. Shepard,⁴⁸ M. Shimojima,^{56,s} S. Shiraishi,¹⁴ M. Shochet,¹⁴ Y. Shon,⁶⁰ I. Shreyber,³⁷ P. Sinervo,³⁴ A. Sisakyan,¹⁶ A. J. Slaughter,¹⁸ J. Slaunwhite,⁴⁰ K. Sliwa,⁵⁷ J. R. Smith,⁸ F. D. Snider,¹⁸ R. Snihur,³⁴ A. Soha,⁸ S. Somalwar,⁵³ V. Sorin,³⁶ T. Spreitzer,³⁴ P. Squillacioti,^{47c,47a} M. Stanitzki,⁶¹ R. St. Denis,²² B. Stelzer,³⁴ O. Stelzer-Chilton,³⁴ D. Stentz,³⁹ J. Strologas,³⁸ G. L. Strycker,³⁵ J. S. Suh,²⁸ A. Sukhanov,¹⁹ I. Suslov,¹⁶ T. Suzuki,⁵⁶ A. Taffard,^{25,g} R. Takashima,⁴¹ Y. Takeuchi,⁵⁶ R. Tanaka,⁴¹ M. Tecchio,³⁵ P. K. Teng,¹ K. Terashi,⁵¹ J. Thom,^{18,i} A. S. Thompson,²² G. A. Thompson,²⁵ E. Thomson,⁴⁶ P. Tipton,⁶¹ P. Tito-Guzmán,³² S. Tkaczyk,¹⁸ D. Toback,⁵⁴ S. Tokar,¹⁵ K. Tollefson,³⁶ T. Tomura,⁵⁶ D. Tonelli,¹⁸ S. Torre,²⁰ D. Torretta,¹⁸ P. Totaro,^{55b,55a} S. Tourneur,⁴⁵ M. Trovato,^{47d,47a} S.-Y. Tsai,¹ Y. Tu,⁴⁶ N. Turini,^{47c,47a} F. Ukegawa,⁵⁶ S. Vallecorsa,²¹ N. van Remortel,^{24,c} A. Varganov,³⁵ E. Vataga,^{47d,47a} F. Vázquez,^{19,o} G. Velev,¹⁸ C. Vellidis,³ M. Vidal,³² R. Vidal,¹⁸ I. Vila,¹² R. Vilar,¹² T. Vine,³¹ M. Vogel,³⁸ I. Volobouev,^{29,v} G. Volpi,^{47b,47a} P. Wagner,⁴⁶ R. G. Wagner,² R. L. Wagner,¹⁸ W. Wagner,^{27,y} J. Wagner-Kuhr,²⁷ T. Wakisaka,⁴² R. Wallny,⁹ S. M. Wang,¹ A. Warburton,³⁴ D. Waters,³¹ M. Weinberger,⁵⁴ J. Weinelt,²⁷ H. Wenzel,¹⁸ W. C. Wester III,¹⁸ B. Whitehouse,⁵⁷ D. Whiteson,^{46,g} A. B. Wicklund,² E. Wicklund,¹⁸ S. Wilbur,¹⁴ G. Williams,³⁴ H. H. Williams,⁴⁶ P. Wilson,¹⁸ B. L. Winer,⁴⁰ P. Wittich,^{18,i} S. Wolbers,¹⁸ C. Wolfe,¹⁴ T. Wright,³⁵ X. Wu,²¹ F. Würthwein,¹⁰ S. Xie,³³ A. Yagil,¹⁰ K. Yamamoto,⁴² J. Yamaoka,¹⁷ U. K. Yang,^{14,f} Y. C. Yang,²⁸ W. M. Yao,²⁹ G. P. Yeh,¹⁸ K. Yi,^{18,p} J. Yoh,¹⁸ K. Yorita,⁵⁸ T. Yoshida,^{42,m} G. B. Yu,⁵⁰ I. Yu,²⁸ S. S. Yu,¹⁸ J. C. Yun,¹⁸ L. Zanello,^{52b,52a} A. Zanetti,^{55a} X. Zhang,²⁵ Y. Zheng,^{9,e} and S. Zucchelli^{6b,6a}

(CDF Collaboration)

¹*Institute of Physics, Academia Sinica, Taipei, Taiwan 11529, Republic of China*²*Argonne National Laboratory, Argonne, Illinois 60439, USA*³*University of Athens, 157 71 Athens, Greece*⁴*Institut de Física d'Altes Energies, Universitat Autònoma de Barcelona, E-08193, Bellaterra (Barcelona), Spain*⁵*Baylor University, Waco, Texas 76798, USA*^{6a}*Istituto Nazionale di Fisica Nucleare Bologna, I-40127 Bologna, Italy*^{6b}*University of Bologna, I-40127 Bologna, Italy*⁷*Brandeis University, Waltham, Massachusetts 02254, USA*⁸*University of California, Davis, Davis, California 95616, USA*⁹*University of California, Los Angeles, Los Angeles, California 90024, USA*¹⁰*University of California, San Diego, La Jolla, California 92093, USA*¹¹*University of California, Santa Barbara, Santa Barbara, California 93106, USA*¹²*Instituto de Física de Cantabria, CSIC-University of Cantabria, 39005 Santander, Spain*¹³*Carnegie Mellon University, Pittsburgh, Pennsylvania 15213, USA*¹⁴*Enrico Fermi Institute, University of Chicago, Chicago, Illinois 60637, USA*¹⁵*Comenius University, 842 48 Bratislava, Slovakia; Institute of Experimental Physics, 040 01 Kosice, Slovakia*¹⁶*Joint Institute for Nuclear Research, RU-141980 Dubna, Russia*¹⁷*Duke University, Durham, North Carolina 27708, USA*¹⁸*Fermi National Accelerator Laboratory, Batavia, Illinois 60510, USA*¹⁹*University of Florida, Gainesville, Florida 32611, USA*²⁰*Laboratori Nazionali di Frascati, Istituto Nazionale di Fisica Nucleare, I-00044 Frascati, Italy*²¹*University of Geneva, CH-1211 Geneva 4, Switzerland*²²*Glasgow University, Glasgow G12 8QQ, United Kingdom*²³*Harvard University, Cambridge, Massachusetts 02138*

- ²⁴*Division of High Energy Physics, Department of Physics, University of Helsinki and Helsinki Institute of Physics, FIN-00014, Helsinki, Finland*
- ²⁵*University of Illinois, Urbana, Illinois 61801, USA*
- ²⁶*The Johns Hopkins University, Baltimore, Maryland 21218, USA*
- ²⁷*Institut für Experimentelle Kernphysik, Universität Karlsruhe, 76128 Karlsruhe, Germany*
- ²⁸*Center for High Energy Physics: Kyungpook National University, Daegu 702-701, Korea; Seoul National University, Seoul 151-742, Korea; Sungkyunkwan University, Suwon 440-746, Korea; Korea Institute of Science and Technology Information, Daejeon, 305-806, Korea; Chonnam National University, Gwangju, 500-757, Korea*
- ²⁹*Ernest Orlando Lawrence Berkeley National Laboratory, Berkeley, California 94720, USA*
- ³⁰*University of Liverpool, Liverpool L69 7ZE, United Kingdom*
- ³¹*University College London, London WC1E 6BT, United Kingdom*
- ³²*Centro de Investigaciones Energeticas Medioambientales y Tecnologicas, E-28040 Madrid, Spain*
- ³³*Massachusetts Institute of Technology, Cambridge, Massachusetts 02139, USA*
- ³⁴*Institute of Particle Physics: McGill University, Montréal, Québec, Canada H3A 2T8; Simon Fraser University, Burnaby, British Columbia, Canada V5A 1S6; University of Toronto, Toronto, Ontario, Canada M5S 1A7; and TRIUMF, Vancouver, British Columbia, Canada V6T 2A3*
- ³⁵*University of Michigan, Ann Arbor, Michigan 48109, USA*
- ³⁶*Michigan State University, East Lansing, Michigan 48824, USA*
- ³⁷*Institution for Theoretical and Experimental Physics, ITEP, Moscow 117259, Russia*
- ³⁸*University of New Mexico, Albuquerque, New Mexico 87131, USA*
- ³⁹*Northwestern University, Evanston, Illinois 60208, USA*
- ⁴⁰*The Ohio State University, Columbus, Ohio 43210, USA*
- ⁴¹*Okayama University, Okayama 700-8530, Japan*
- ⁴²*Osaka City University, Osaka 588, Japan*
- ⁴³*University of Oxford, Oxford OX1 3RH, United Kingdom*
- ^{44a}*Istituto Nazionale di Fisica Nucleare, Sezione di Padova-Trento, I-35131 Padova, Italy*
- ^{44b}*University of Padova, I-35131 Padova, Italy*
- ⁴⁵*LPNHE, Universite Pierre et Marie Curie/IN2P3-CNRS, UMR7585, Paris, F-75252 France*
- ⁴⁶*University of Pennsylvania, Philadelphia, Pennsylvania 19104, USA*
- ^{47a}*Istituto Nazionale di Fisica Nucleare Pisa, I-56127 Pisa, Italy*
- ^{47b}*University of Pisa, I-56127 Pisa, Italy*
- ^{47c}*University of Siena, I-56127 Pisa, Italy*
- ^{47d}*Scuola Normale Superiore, I-56127 Pisa, Italy*
- ⁴⁸*University of Pittsburgh, Pittsburgh, Pennsylvania 15260, USA*
- ⁴⁹*Purdue University, West Lafayette, Indiana 47907, USA*
- ⁵⁰*University of Rochester, Rochester, New York 14627, USA*
- ⁵¹*The Rockefeller University, New York, New York 10021, USA*
- ^{52a}*Istituto Nazionale di Fisica Nucleare, Sezione di Roma 1, I-00185 Roma, Italy*
- ^{52b}*Sapienza Università di Roma, I-00185 Roma, Italy*
- ⁵³*Rutgers University, Piscataway, New Jersey 08855, USA*
- ⁵⁴*Texas A&M University, College Station, Texas 77843, USA*
- ^{55a}*Istituto Nazionale di Fisica Nucleare Trieste/Udine, I-34100 Trieste, Italy*
- ^{55b}*University of Trieste/Udine, I-33100 Udine, Italy*
- ⁵⁶*University of Tsukuba, Tsukuba, Ibaraki 305, Japan*
- ⁵⁷*Tufts University, Medford, Massachusetts 02155, USA*
- ⁵⁸*Waseda University, Tokyo 169, Japan*
- ⁵⁹*Wayne State University, Detroit, Michigan 48201, USA*
- ⁶⁰*University of Wisconsin, Madison, Wisconsin 53706, USA*
- ⁶¹*Yale University, New Haven, Connecticut 06520, USA*
- (Received 17 March 2009; published 4 June 2009)

We report on a search for the supersymmetric partner of the bottom quark produced from gluino decays in data from 2.5 fb^{-1} of integrated luminosity collected by the Collider Detector at Fermilab at $\sqrt{s} = 1.96 \text{ TeV}$. Candidate events are selected requiring two or more jets and large missing transverse energy. At least two of the jets are required to be tagged as originating from a b quark to enhance the sensitivity. The results are in good agreement with the prediction of the standard model processes, giving no evidence for gluino decay to bottom squarks. This result constrains the gluino-pair-production cross section to be less than 40 fb at 95% credibility level for a gluino mass of $350 \text{ GeV}/c^2$.

The standard model (SM) of elementary particles and fundamental interactions, however successful, is incomplete, since it does not explain the origin of electroweak symmetry breaking or the gauge hierarchy problem [1]. A proposed extension of the SM, supersymmetry (SUSY) [2], solves these problems by introducing a symmetry that relates particles of different spin. R -parity [2] conserving SUSY models also provide a prime candidate for the dark matter in the cosmos [3], namely, the stable lightest supersymmetric particle (LSP). In these models, the left-handed and right-handed quarks have scalar partners denoted \tilde{q}_L and \tilde{q}_R which can mix to form scalar quarks (squarks) with mass eigenstates $\tilde{q}_{1,2}$. Several models [4] predict that this mixing can be substantial for the scalar bottom (bottom squark), yielding a bottom-squark mass eigenstate (\tilde{b}), significantly lighter than other squarks. In proton-antiproton ($p\bar{p}$) collisions at the Tevatron's center-of-mass energy of $\sqrt{s} = 1.96$ TeV, the gluino (\tilde{g} , the spin-1/2 superpartner of the gluon) pair-production cross section is almost an order of magnitude larger than that of a bottom squark of similar mass [5]. Therefore, if sufficiently light, sbottom quarks could be copiously produced through the $\tilde{g} \rightarrow \tilde{b}b$ decays since the gluino preferentially decays into a squark-quark pair [2]. A sbottom in the mass range accessible at the Tevatron is expected to decay predominantly into a bottom quark and the lightest neutralino ($\tilde{\chi}^0$), which is often assumed to be the LSP. Previous searches for direct sbottom [6,7] or gluino production [8,9] at the Tevatron placed lower limits on the masses of these particles.

In this Letter, we report the search for $\tilde{g} \rightarrow \tilde{b}b$ decays in $p\bar{p}$ collision data from 2.5 fb^{-1} of integrated luminosity collected between March 2003 and April 2008 by the upgraded Collider Detector at Fermilab (CDF II) at the Tevatron. Assuming R -parity conservation, \tilde{g} 's are produced in pairs. We consider a scenario where the branching fractions $\tilde{g} \rightarrow b\tilde{b}$ and $\tilde{b} \rightarrow b\tilde{\chi}^0$ are 100%. If these conditions are satisfied the analysis is largely independent of the $\tilde{\chi}^0$ mass, as long as the $m(\tilde{b}) - m(\tilde{\chi}^0)$ is larger than $25 \text{ GeV}/c^2$, due to b -jet energy cut (to be discussed later). For our calculations we assume a $\tilde{\chi}^0$ mass of $60 \text{ GeV}/c^2$, which is above the limits from LEP [10]. The final state contains four b jets from the hadronization of the b quarks and an imbalance in momentum in the transverse plane to the beam ("missing transverse energy" or \cancel{E}_T [11]) from the two undetected LSPs.

CDF II is a multipurpose detector, described in detail elsewhere [12]. The charged-particle tracking system consists of silicon microstrip detectors and a cylindrical open-cell drift chamber in a 1.4 T solenoidal magnetic field coaxial with the beam line. The silicon detectors provide coverage in the pseudorapidity [11] range $|\eta| \leq 2$ and are used to identify events with long-lived particle decays. The

drift chamber surrounds the silicon detectors and has maximum efficiency up to $|\eta| = 1$. Segmented sampling calorimeters, arranged in a projective tower geometry, surround the tracking system, and measure the energy of interacting particles for $|\eta| \leq 3.6$. Muons are identified by drift chambers, which extend to $|\eta| = 1.5$, and are located outside the calorimeter volume. Jets are reconstructed from the energy depositions in the calorimeter cells using an iterative cone jet-clustering algorithm [13], with a cone size of radius $R = \sqrt{(\Delta\phi)^2 + (\Delta\eta)^2} = 0.4$ [11]. Energy corrections [14] are applied to account for effects that distort the measured jet energy, such as nonlinear calorimeter response, underlying event, and the position of the primary vertex.

Candidate events used for this search are selected by an online event selection system, a (trigger) requiring $\cancel{E}_T \geq 45 \text{ GeV}$. Further selections remove accelerator-produced and detector-related backgrounds as well as cosmic-ray events. After offline event reconstruction, the events are required to have $\cancel{E}_T \geq 70 \text{ GeV}$, and at least two jets with $|\eta| \leq 2.4$ and $E_T \geq 25 \text{ GeV}$. The highest- E_T jet is required to have $E_T \geq 35 \text{ GeV}$ and at least one of the selected jets is required to have $|\eta| \leq 0.9$. The B hadrons in jets coming from b quark fragmentation have an average flight path of about 500 microns, yielding secondary vertices relative to the interaction point (primary vertex). We require the events to have at least two jets identified as b jets by the CDF secondary-vertex b -tagging algorithm [15]. The double b -tagging requirement effectively enhances the sensitivity.

Dominant SM backgrounds are top-quark pair-production and single top-quark production, electroweak boson and diboson production, heavy-flavor (HF) multijet production, and light-flavor jets falsely tagged as b jets (mistags). The latter two background contributions are estimated from data. The PYTHIA event generator [16] is used to estimate the remaining backgrounds. For the event generation the CTEQ5L [17] parton distribution functions were used. Events are passed through the GEANT3-based [18] CDF II detector simulation [19] and weighted by the probability that they would pass the trigger as determined in independent data samples. The single top-quark and diboson event yields are normalized to the theoretical cross sections [20–22]. The event yields for the electroweak boson samples are normalized to the leading order cross section provided by PYTHIA, scaled by a factor of 1.4 to account for higher-order corrections. We use the top-quark pair production cross section of $\sigma_{t\bar{t}} = 7.3 \pm 0.8 \text{ pb}$ [23]. Mistags are estimated from inclusive jet-sample data by computing a mistag rate [15] which is parametrized by the jet E_T , $|\eta|$, secondary-vertex track-multiplicity, the number of primary vertices in the event, primary vertex z position, and the scalar sum of E_T of all jets in the event.

To estimate the HF multijet background from data, we have developed a multijet tag-rate estimator (MUTARE). The estimator is based on a tag-rate matrix applied to each jet in an event following a parametrization of E_T , $|\eta|$ and the scalar sum of E_T of all jets in the event. Each element of the matrix is computed in a reference sample as the ratio between the number of b -tagged jets minus the number of mistags over the number of “taggable” jets, where taggable jets are defined as jets with tracks passing the CDF secondary-vertex b -tagging algorithm requirements [15]. The final prediction is obtained after subtracting the HF contribution coming from nonmultijet production processes. The amount of nonmultijet HF contribution is computed by applying the MUTARE matrix to each nonmultijet background sample described above.

To avoid potential biases when searching for new physics, we test the various background contributions in distinct control regions that are defined *a priori*. The three control regions used to check the SM prediction are denoted as multijet, lepton, and preoptimization regions. The multijet control region is defined to have the second leading E_T jet (\vec{j}_2) aligned with the $\vec{\cancel{E}}_T$ [11], where aligned means $\Delta\phi(\vec{\cancel{E}}_T, \vec{j}_2) \leq 0.4$ rad. This HF multijet enriched region is used to build the MUTARE matrix to predict the HF multijet background in the other control and signal regions. The lepton control region is defined to have \vec{j}_2 not aligned with the $\vec{\cancel{E}}_T$ ($\Delta\phi(\vec{\cancel{E}}_T, \vec{j}_2) \geq 0.7$ rad) and at least one isolated lepton with $p_T \geq 10$ GeV/ c . This lepton region is used to check the top quark and electroweak W/Z boson backgrounds. The preoptimization control region is defined to have the leading and second-leading E_T jets not aligned with the $\vec{\cancel{E}}_T$ and to have no identified leptons. Predicted total numbers of events and distributions of kinematic variables such as jet E_T , the track multiplicity, and the \cancel{E}_T have been studied and found to be in agreement with observations in the three control regions. As an example, the \cancel{E}_T distributions for the preoptimization region are shown in Fig. 1. The background contributions to the number of expected inclusive double b -tagged events and the observed events in the control regions are summarized in Table I.

We optimize the sensitivity to bottom-squark production from gluino decays by using two neural networks (NN) trained with the TMVA package [24]. One of them is optimized to remove the HF multijet background (multijet-NN) and the other to remove the top-quark pair background (top-NN). The training is based on jet variables using, jet E_T , $\Delta\phi(\vec{\cancel{E}}_T, \vec{j}_i)$, \cancel{E}_T , and the summed E_T of all the jets in the event. We choose two reference signal points based on values of $\Delta m \equiv m(\tilde{g}) - m(\tilde{b})$ and perform the same optimization procedure. We refer to large Δm optimization with $m(\tilde{g}) = 335$ GeV/ c^2 and $m(\tilde{b}) = 260$ GeV/ c^2 and to small Δm optimization with $m(\tilde{g}) = 335$ GeV/ c^2 and $m(\tilde{b}) = 315$ GeV/ c^2 . These two signal

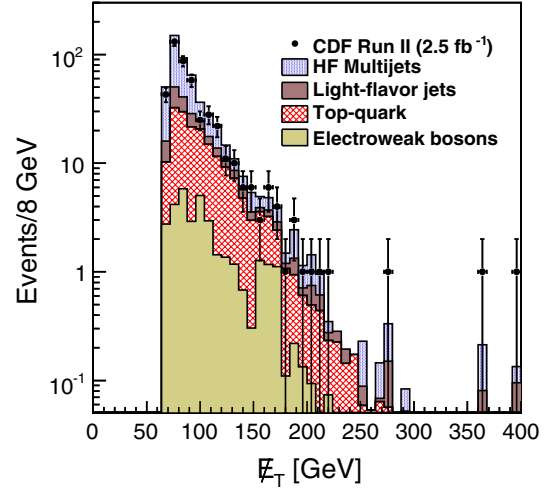


FIG. 1 (color online). Distribution of \cancel{E}_T in the preoptimization region in which leading E_T and second-leading E_T jets are not aligned with the \cancel{E}_T , and isolated leptons are vetoed. SM prediction (stacked histograms) and observed distribution (dots) are shown, where HF multijets and light-flavor jets are predicted from data as an integrated estimation.

points represent two different kinematic regions. For the large Δm optimization three or more jets are required before applying the NN procedure. For the small Δm optimization two or more jets are required since the E_T spectrum of the b jets is much softer. The signal predictions are obtained by computing the acceptance using the PYTHIA event generator normalized to the NLO production cross section determined with PROSPINO event generator [5] and the CTEQ6M [25,26] parton distribution functions. The uncertainty of the NLO production cross section varies from 20% [$m(\tilde{g}) \approx 200$ GeV/ c^2] to 30% [$m(\tilde{g}) \approx 400$ GeV/ c^2].

The systematic uncertainties on the signal and the background predictions, taking into account correlated and uncorrelated uncertainties, are studied. Correlated uncertainties, affecting both the background prediction and signal acceptance, are dominated by the jet energy scale [16% (25%) [14] for the large (small) Δm optimization region], the different b -tagging efficiency between data and simulation [4.4% (4.9%) [15] for the large (small) Δm optimi-

TABLE I. Comparison of the total number of expected events with total uncertainties and observed double b -tagged events in the control regions.

Regions:	Multijet	Lepton	Preoptimization
Electroweak bosons	10 ± 7	21 ± 14	33 ± 22
Top-quark	19 ± 6	111 ± 34	146 ± 45
Light-flavor jets	225 ± 49	8 ± 2	57 ± 12
HF Multijets	839 ± 419	25 ± 12	270 ± 135
Total expected	1093 ± 422	165 ± 39	506 ± 144
Observed	1069	159	451

TABLE II. Number of expected and observed events in the signal regions. Predictions for the signal points are also shown. Correlated and uncorrelated uncertainties in the total background and expected signal were treated separately in the analysis although they are combined here.

Optimizations:	Large Δm	Small Δm
Electroweak bosons	0.17 ± 0.05	0.5 ± 0.3
Top-quark	1.9 ± 1.0	0.6 ± 0.4
Light-flavor jets	1.0 ± 0.3	0.6 ± 0.1
HF Multijets	1.6 ± 0.8	0.7 ± 0.3
Total expected SM	4.7 ± 1.5	2.4 ± 0.8
Observed	5	2
Optimized \tilde{g} signal	14.9 ± 5.0	8.5 ± 2.8

zation region], and the luminosity (6%) [12]. Uncorrelated systematic uncertainties on the background predictions are dominated by the HF multijet b -tag rate (50%), the mistag rate (16% [15] for light-flavor multijets), the top-quark pair-production cross section (11%), the single top-quark production cross section (13%), and the diboson production cross section (10% for WW/WZ and 20% for ZZ). Because of the limited ability of PYTHIA to simulate multijet environments, a 40% uncertainty [27] is assigned for the extracted yields of events with a W or Z boson and jets. Correlated and uncorrelated uncertainties are evaluated separately and combined in quadrature.

The signal region is analyzed after the background predictions are determined. We find 0.8 as an optimal value for the selection cut for both multijet-NN outputs and 0.6 (0.8) for the top-NN outputs in the large (small) Δm optimization within an interval of -1 to 1 , where the

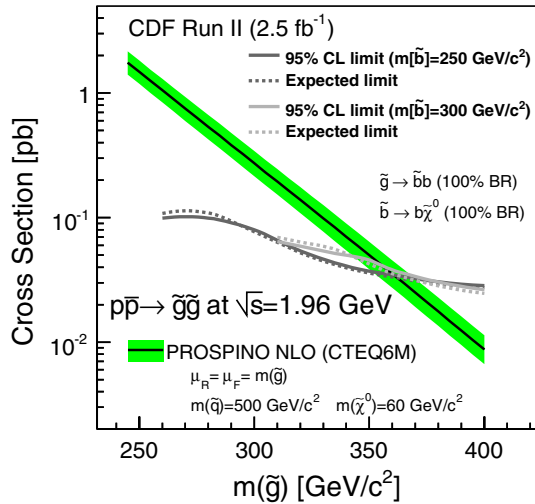


FIG. 2 (color online). Observed (solid lines) and expected (dashed lines) 95% C.L. upper limit on the gluino cross section (solid line with band) as a function of the gluino mass for two assumed values of the sbottom mass. The shaded band denotes the uncertainty on the NLO $\tilde{g}\tilde{g}$ production due to the truncated higher-order terms and the parton distribution functions.

background peaks at -1 and the signal peaks at 1 . We observe 5 (2) events for the large (small) Δm optimization region, where 4.7 ± 1.5 (2.4 ± 0.8) are expected from background, as summarized in Table II. Since no significant deviation from the SM prediction is observed, the results are used to calculate an exclusion limit for the cross section of the described gluino process. We use a Bayesian method to determine the 95% credibility level (C.L.) upper limit on the $\tilde{g}\tilde{g}$ cross section, assuming a uniform prior probability density. We treat the various correlated uncertainties as nuisance parameters, which we remove by marginalization, assuming a Gaussian prior distribution. The obtained limit is such that no more than 8.0 (5.4) events are observed in the large (small) Δm signal region. Figure 2 shows the expected and observed limits as a function of $m(\tilde{g})$ for two values of the \tilde{b} quark mass. The expected limit is computed by assuming that the observed number of events matches the SM expectation in each signal region.

The gluino production cross section limit is nearly independent of the bottom-squark mass between 250 and 300 GeV/c^2 , and is around 40 fb for $m(\tilde{g}) = 350 \text{ GeV}/c^2$. In addition, using the assumed model, a 95% C.L. limit is obtained in the parameter plane of the model. Figure 3 shows the excluded region in the gluino-bottom-squark mass plane, compared with the results from previous analyses [6–9]. The limit obtained with the present analysis improves the results of previous searches using similar topology and also, under the assumptions discussed above, sets a more stringent limit on the sbottom and gluino production than dedicated sbottom searches.

In conclusion, we have searched for sbottom quarks from gluino decays in 2.5 fb^{-1} of CDF Run II data. We observe 5 (2) inclusive double b -tagged candidate events

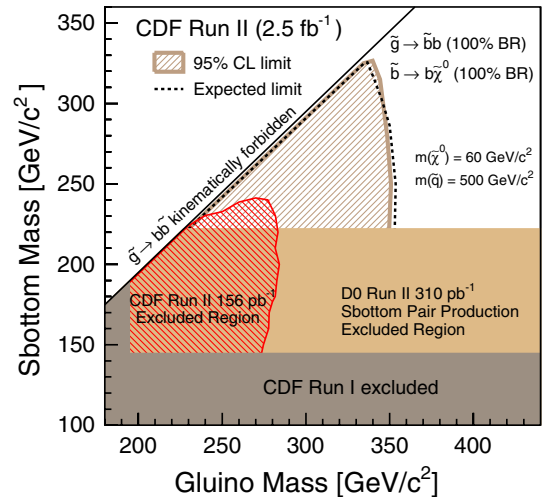


FIG. 3 (color online). Excluded region at 95% C.L. in the $m(\tilde{g})$ - $m(\tilde{b})$ plane for a $m(\tilde{\chi}^0) = 60 \text{ GeV}/c^2$, $m(\tilde{q}) = 500 \text{ GeV}/c^2$. The result is compared to the previous results from CDF in run I [8], and run II [9] and direct sbottom production by D0 [7].

for the large (small) Δm optimization region, which is in agreement with SM background expectations of 4.7 ± 1.5 (2.4 ± 0.8) events. No evidence for sbottom quarks from gluino decays is observed, and we exclude a significant region in the gluino and sbottom mass plane at 95% C.L. For the assumed model, the limit is nearly independent of the sbottom mass and the cross section limit is around 40 fb for $m(\tilde{g}) = 350 \text{ GeV}/c^2$.

We thank the Fermilab staff and the technical staffs of the participating institutions for their vital contributions. This work was supported by the U.S. Department of Energy and National Science Foundation; the Italian Istituto Nazionale di Fisica Nucleare; the Ministry of Education, Culture, Sports, Science and Technology of Japan; the Natural Sciences and Engineering Research Council of Canada; the National Science Council of the Republic of China; the Swiss National Science Foundation; the A.P. Sloan Foundation; the Bundesministerium für Bildung und Forschung, Germany; the Korean Science and Engineering Foundation and the Korean Research Foundation; the Science and Technology Facilities Council and the Royal Society, UK; the Institut National de Physique Nucleaire et Physique des Particules/CNRS; the Russian Foundation for Basic Research; the Ministerio de Ciencia e Innovación, and Programa Consolider-Ingenio 2010, Spain; the Slovak R&D Agency; and the Academy of Finland.

^aDeceased.

^bVisitor from University of Massachusetts Amherst, Amherst, MA 01003, USA.

^cVisitor from Universiteit Antwerpen, B-2610 Antwerp, Belgium.

^dVisitor from University of Bristol, Bristol BS8 1TL, United Kingdom.

^eVisitor from Chinese Academy of Sciences, Beijing 100864, China.

^fVisitor from Istituto Nazionale di Fisica Nucleare, Sezione di Cagliari, 09042 Monserrato (Cagliari), Italy.

^gVisitor from University of California Irvine, Irvine, CA 92697, USA.

^hVisitor from University of California Santa Cruz, Santa Cruz, CA 95064, USA.

ⁱVisitor from Cornell University, Ithaca, NY 14853, USA.

^jVisitor from University of Cyprus, Nicosia CY-1678, Cyprus.

^kVisitor from University College Dublin, Dublin 4, Ireland.

^lVisitor from University of Edinburgh, Edinburgh EH9 3JZ, United Kingdom.

^mVisitor from University of Fukui, Fukui City, Fukui Prefecture, Japan 910-0017.

ⁿVisitor from Kinki University, Higashi-Osaka City, Japan 577-8502.

^oVisitor from Universidad Iberoamericana, Mexico D.F., Mexico.

^pVisitor from University of Iowa, Iowa City, IA 52242, USA.

^qVisitor from Queen Mary, University of London, London, E1 4NS, England.

^rVisitor from University of Manchester, Manchester M13 9PL, England.

^sVisitor from Nagasaki Institute of Applied Science, Nagasaki, Japan.

^tVisitor from University of Notre Dame, Notre Dame, IN 46556, USA.

^uVisitor from University de Oviedo, E-33007 Oviedo, Spain.

^vVisitor from Texas Tech University, Lubbock, TX 79609, USA.

^wVisitor from IFIC(CSIC-Universitat de Valencia), 46071 Valencia, Spain.

^xVisitor from University of Virginia, Charlottesville, VA 22904, USA.

^yVisitor from Bergische Universität Wuppertal, 42097 Wuppertal, Germany.

^zOn leave from J. Stefan Institute, Ljubljana, Slovenia.

- [1] E. Gildener, Phys. Rev. D **14**, 1667 (1976).
- [2] For a review of SUSY, see S.P. Martin, arXiv:hep-ph/9709356, and references therein.
- [3] H. Goldberg, Phys. Rev. Lett. **50**, 1419 (1983); J. Ellis, J. Hagelin, D. Nanopoulos, K. Olive, and M. Srednicki, Nucl. Phys. **B238**, 453 (1984).
- [4] A. Bartl, W. Majerotto, and W. Porod, Z. Phys. C **64**, 499 (1994); **68**, 518(E) (1995).
- [5] W. Beenakker, R. Hopker, M. Spira, and P.M. Zerwas, Nucl. Phys. **B492**, 51 (1997); W. Beenakker, R. Hopker, and M. Spira, arXiv:hep-ph/9611232. We use PROSPINO 1.0.
- [6] T. Affolder *et al.* (CDF Collaboration), Phys. Rev. Lett. **84**, 5704 (2000).
- [7] V.M. Abazov *et al.* (D0 Collaboration), Phys. Rev. Lett. **97**, 171806 (2006).
- [8] T. Affolder *et al.* (CDF Collaboration), Phys. Rev. Lett. **88**, 041801 (2002).
- [9] A. Abulencia *et al.* (CDF Collaboration), Phys. Rev. Lett. **96**, 171802 (2006).
- [10] LEPSUSYWG/04-07.1, <http://lepsusy.web.cern.ch/lepsusy/>.
- [11] We use a cylindrical coordinate system with its origin at the center of the detector, where θ and ϕ are the polar and azimuthal angles, respectively, and pseudorapidity is $\eta = -\ln(\tan(\frac{\theta}{2}))$. The missing E_T (\cancel{E}_T) is defined by $\cancel{E}_T = -\sum_i E_T^i \hat{n}_i$, $i =$ calorimeter tower number, where \hat{n}_i is a unit vector perpendicular to the beam axis and pointing at the i th calorimeter tower. \cancel{E}_T is corrected for high-energy muons and jet energy. We define $\cancel{E}_T = |\cancel{E}_T|$.
- [12] D. Acosta *et al.* (CDF Collaboration), Phys. Rev. D **71**, 032001 (2005).
- [13] G. Arnison *et al.* (UA1 Collaboration), Phys. Lett. B **123**, 115 (1983); A. Bhatti *et al.*, Nucl. Instrum. Methods Phys. Res., Sect. A **566**, 375 (2006).
- [14] A. Bhatti *et al.* (CDF Collaboration), Nucl. Instrum. Methods Phys. Res., Sect. A **566**, 375 (2006).

- [15] D. Acosta *et al.* (CDF Collaboration), Phys. Rev. D **71**, 052003 (2005).
- [16] T. Sjöstrand *et al.*, Comput. Phys. Commun. **135**, 238 (2001). We use PYTHIA version 6.216.
- [17] H.L. Lai *et al.*, Eur. Phys. J. C **12**, 375 (2000).
- [18] R. Brun *et al.*, CERN Tech. Report No. CERN-DD/EE/84.1, 1987.
- [19] E. Gerchtein and M. Paulini, *Computing in High Energy and Nuclear Physics 2003 Conference Proceedings*, eConf C0303241, TUMT005 (2003).
- [20] B.W. Harris *et al.*, Phys. Rev. D **66**, 054024 (2002); Z. Sullivan, Phys. Rev. D **70**, 114012 (2004).
- [21] M. Cacciari *et al.*, J. High Energy Phys. 04 (2004) 068.
- [22] J.R. Campbell and R.K. Ellis, Phys. Rev. D **60**, 113006 (1999).
- [23] L. Cerrito, in *Proceedings of the Heavy Quarks and Leptons, Munich, Germany, 2006*, edited by S. Recksiegel, A. Hoang, and S. Paul, eConf C0610161, 459 (2006).
- [24] A. Hocker *et al.*, arXiv:physics/0703039.
- [25] J. Pumplin *et al.*, J. High Energy Phys. 07 (2002) 012.
- [26] D. Stump *et al.*, J. High Energy Phys. 10 (2003) 046.
- [27] T. Aaltonen *et al.* (CDF Collaboration), Phys. Rev. Lett. **100**, 211801 (2008).